Hindawi

*Research Article*

# Study on Dynamics of Hydraulic Control System for Automatic Loading and Unloading of Drill Pipe of Geological Drilling Rig

**Zhijian Liu** (ID)**, Yunlong Chen** (ID)**, and Hailong Ruan** (ID)

*Beijing Institute of Exploration Engineering, CGS, Beijing, China*

Correspondence should be addressed to Hailong Ruan; rhailong@mail.cgs.gov.cn

With the increasing demand for resources, the task of the geological survey is growing rapidly. The automatic geological drilling rig, which can improve the efficiency of the geological survey, has become the mainstream development direction. In this study, the hydraulic control system for the automatic screw up and screw down of an automatic drilling rig is studied. Through the establishment of mathematical models such as the four-way slide valve controlled asymmetric cylinder model, drill pipe thread stress model, and steel wire rope elastic model, the hydraulic valve is used to limit the pressure of the hydraulic cylinder, closed-loop control to control rotation speed, and power head floating to prevent screw damage and realize the automatic control of drill pipe up and down of a geological drilling rig. The hydraulic control system is simulated by AMESim software. The simulation model verifies the mathematical model. It is concluded that the maximum transient force of steel wire rope is caused by the elastic coefficient K of steel wire rope, but the magnitude is independent of K. The transient force is the periodic motion force. The displacement, velocity, and acceleration of load are periodic functions related to time. By installing a small flow load sensing valve, the displacement of an asymmetric hydraulic cylinder can be accurately controlled, and then, the displacement of the drilling rig powerhead can be controlled. The combined action of drill pipe speed and power head displacement is adopted, and the power head displacement is followed by PID control through the feedback value of the drill pipe speed, which can realize the automatic loading and unloading of drill pipe and reduce the damage of drill pipe screw during loading and unloading of drill pipe. The research results of this study can provide a theoretical reference and design basis for the follow-up development of an automatic drilling rig.

## 1. Introduction

Both oil drilling and geological core drilling obtain mineral resources by drilling, and this will still be the main construction method in the next few decades. In the process of drilling, the drill pipe string, as the main drilling mechanism, plays an important role in transmitting force and as a drilling mud channel [1]. Therefore, in order to realize automatic loading and unloading of drill pipes, especially the use of rope-coring drill pipes, there is an insurmountable problem of the screw thread on the drill pipe. When the screw thread is unloaded from the drill pipe, the power head shall be lowered (or lifted) by a pitch while rotating forward (or reverse) one turn. In the process of tightening the thread, the eccentricity of the internal and external threads will cause

thread wear or burning, and the insufficient or excessive make-up torque during thread tightening will affect the service life of the joint thread. Most drill pipe thread failures occur from the root of the external thread to the second circle. The main forms of thread failure are wear, root fracture, or longitudinal cracking [2]. Research shows that the failure position of the drill pipe is mainly concentrated in the position of drill pipe joint and thread. In the study of drill pipe stress characteristics, the failure caused by joint thread accounts for about 48% of the total failure of drilling tools [3].

At present, A. R. Shahani and S.M.H. Sharifi [4] have carried out nonlinear finite element contact analysis on threaded structures. Santus C et al. [5] studied the calculation methods of force for hot and cold installation of drill

pipe joint in view of the engineering problems caused by unreasonable screwing up of drill pipe joints. Van Wittenbergh et al. [6] studied the influence of thread contact parameters of the drill pipe joint of the API structure on contact stress by a series of finite element calculation methods and experimental methods and pointed out that the first meshing tooth of male buckle is the most dangerous position for fatigue failure. Croccolo et al. [7] analyzed the causes of joint thread failure of ordinary bolts after torque preloading and the relationship between friction coefficient and make-up torque. Bui et al. [8] established a fatigue life judgment model, which can be used to judge the antifatigue life of large pipe fittings. Research on drill pipe joint thread at home and abroad mainly focuses on the research on thread structure, stress-strain concentration of joint threads, and failure analysis of joint thread. How to prevent and reduce the impact of drill pipe, especially the elastic impact of drill pipe, is also a hot issue in the research of drill pipe drill string [9], but there is little research on the dynamics of the hydraulic control system when the drill pipe thread is screwed on and off.

Starting with the principle of the hydraulic system of loading and unloading drill pipe, this study establishes the four-way slide valve controlled asymmetric cylinder model, the drill pipe thread stress model, and the steel wire rope elastic model, respectively. Taking the parameters of a certain type of drilling rig as the boundary conditions, the dynamics of the hydraulic control system in the process of loading and unloading drill pipe is deeply studied by using simulation software.

## 2. Closed-Loop Control of Loading and Unloading Drill Pipe

When the automatic drilling rig system completes the process of loading and unloading the drill pipe, it is necessary to realize the screw up and down between the two drill pipes so as to ensure that the drill pipe thread will not be damaged in the process of loading and unloading. When loading and unloading the drill pipe screw thread, the feed oil cylinder shall cooperate with the lifting while the power head rotates to ensure that the power head rotates for one cycle and the feed oil cylinder rises or falls by one pitch.

*2.1. Overload Control.* The feed cylinder is an actuator that acts on the power head, applies an axial force to the drill pipe, and lifts or lowers the power head. In the process of deep drilling, when the pressure of the feed cylinder is overpressured, the drill pipe will be bent and elastically deformed, resulting in the damage of the drill pipe. At the same time, too high pressure will easily lead to the deviation of the drill bit from the predetermined track.

The feed cylinder outputs pressure or lifting force through hydraulic oil applied to the rod chamber or nonrod chamber. Therefore, the pressure and lifting force can be controlled by controlling the pressure in both chambers of the feed cylinder. The pressure control of the feed cylinder adopts a load-sensitive feedback pressure limit to control the

pressure of two chambers of the feed cylinder. Overload control can effectively protect the drill pipe and drill pipe thread buckle.

*2.2. Floating Control of Loading and Unloading Drill Pipe.* The floating control of loading and unloading drill pipe of the geological drilling rig is mainly to avoid the damage of drill pipe thread caused by the weight of power head when loading and unloading drill pipe. The hydraulic principle is shown in Figure 1. The hydraulic system of the drilling rig power head is composed of main system and floating system. The normal drilling and lifting of the drilling rig are controlled by the main system, and the direction and output flow of the main valve 13 are controlled by the manual proportional pilot valve 16, so as to control the drilling and lifting of the power head and its speed. The safety pressures at the lifting side and the lowering side of the power head are set by the lifting side safety valve 14 and the lowering side safety valve 15, and the balance valve 22 ensures the stability of the power head during lifting, lowering, and hovering.

When the drill pipe is required to make up and break down during tripping, the lifting cylinder of the pipe grabbing manipulator and the feed cylinder of the drill power head need to be matched synchronously with the rotating speed of the drill power head and follow the closed-loop control with the rotating speed of the power head. In the process of drilling rig control, the output shaft of the power head rotates for one cycle, and the power head lifts or lowers a drill pipe pitch to ensure that the drill pipe thread is not affected by the dead weight of the power head. This process is called power head floating control.

The rotary encoder installed at the output shaft of the power head measures the rotation direction and speed of the power head. After collecting the data, the controller compares it with the target direction and speed and controls the valve core displacement of the proportional direction valve 11 by controlling the control current of the electric proportional reducing valve 4 on the lifting side and the electric proportional reducing valve 1 on the pressurizing side of the power head. Then, the output flow and direction of the proportional directional valve are controlled, by controlling the direction and opening of proportional directional valve 11 (flow area, approximately linear ratio with displacement), then controlling the direction and speed of the oil cylinder, finally realizing the follow-up control of power head lifting or lowering, and completing the task of loading and unloading drill pipe.

## 3. Modeling Analysis

*3.1. Four-Way Valve Controlled Asymmetric Cylinder Model.* The feed cylinder is a typical four-way spool valve controlled asymmetric hydraulic cylinder. Now, the four-way valve controlled asymmetric hydraulic cylinder is modeled and analyzed to provide a theoretical basis for simulation. The principle of a valve controlled asymmetric hydraulic cylinder is shown in Figure 2.
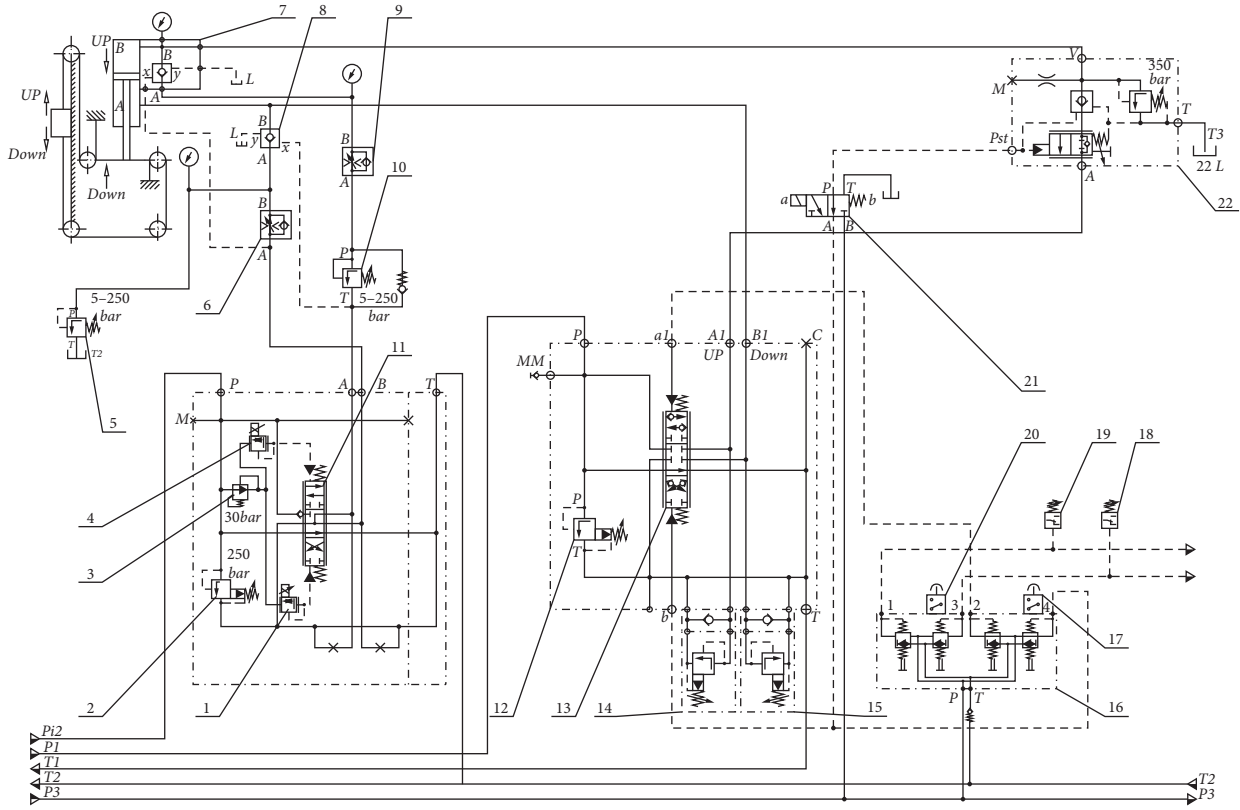
FIGURE 1: Schematic diagram of power head floating control [10].

The flow equation of the four-way slide valve is shown as

$$
q_{sv1} = \begin{cases} 0, & x_v < \Delta_1, \\[2mm] C_d A_{sv1} \sqrt{\dfrac{2}{\rho}\left(p_s - p_1\right)}, & x_v > \Delta_1, \end{cases}
$$

$$
q_{sv2} = \begin{cases} 0, & x_v < -\Delta_2, \\[2mm] C_d A_{sv2} \sqrt{\dfrac{2}{\rho}\left(p_s - p_2\right)}, & x_v > -\Delta_2, \end{cases}
$$

$$
q_{sv3} = \begin{cases} 0, & x_v < \Delta_3, \\[2mm] C_d A_{sv3} \sqrt{\dfrac{2}{\rho}\left(p_s - p_3\right)}, & x_v > \Delta_3, \end{cases}
$$

$$
q_{sv4} = \begin{cases} 0, & x_v < -\Delta_4, \\[2mm] C_d A_{sv4} \sqrt{\dfrac{2}{\rho}\left(p_s - p_4\right)}, & x_v > -\Delta_4, \end{cases}
$$

$$(1)$$
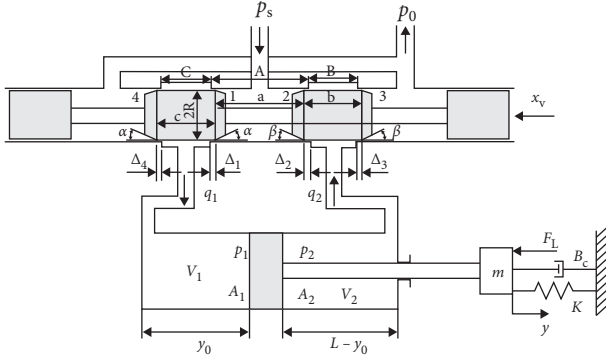
FIGURE 2: Principle of a four-way valve controlled asymmetric hydraulic cylinder [11].



FIGURE 3: Stress analysis of drill pipe thread.

where $C_d$ is the flow coefficient of the valve, $p_s$ is the valve inlet pressure, $q_{svi}$ is the flow through the $i$th valve port, $i = 1 \sim 4$, and $A_{svi}$ is the flow area through the $i$th valve port, $i = 1 \sim 4$.

It can be seen from Figure 2 that the flow in and out of the two chambers of the hydraulic cylinder is shown in following equation:

$$q_1 = f_1(x_v, p_1) = q_{sv1} - q_{sv4},$$
$$q_2 = f_2(x_v, p_2) = q_{sv3} - q_{sv3}. \tag{2}$$

Equations (3) and (4) are continuity equations of the hydraulic cylinder:

$$\dot{p}_1 = \frac{\beta_e}{V_1(y)} \left[ q_1 - C_{ic}(p_1 - p_2) - A_1 \dot{y} \right], \tag{3}$$

$$\dot{p}_2 = \frac{\beta_e}{V_2(y)} \left[ -q_2 - C_{ic}(p_1 - p_2) - C_{ec}p_2 - A_2 \dot{y} \right], \tag{4}$$

where $V_1(y) = A_1(y_0 + y) + V_{d1}$ and $V_2(y) = A_2(L - y_0 - y) + V_{d2}$, $L$ is the stroke of hydraulic cylinder, $\beta_e$ is the bulk modulus of the working medium, $C_{ic}$ and $C_{ec}$ are internal leakage coefficient and external leakage coefficient, and $V_{d1}$ and $V_{d2}$ are the dead cavity volumes of rodless cavity and rodless cavity independent of stroke.

Equation (5) is the force balance equation of hydraulic cylinder and load:

$$A_1 p_1 - A_2 p_2 = m\ddot{y} + B_c\dot{y} + ky + F_L, \tag{5}$$

where $m$ is the total mass of piston and load, $B_c$ is the viscous damping coefficient of the piston and load, $K$ is the load spring stiffness, and $F_L$ is the load force.

The mathematical dynamic characteristic equation of valve controlled asymmetric hydraulic cylinder is shown in the following equations:

$$\dot{x}_1 = x_2,$$

$$\dot{x}_2 = \frac{1}{m}(A_1 x_3 - A_2 x_4 - B_c x_2 - kx_1 - F_L),$$

$$\dot{x}_3 = \frac{1}{A_1(y_0 + x_1) + V_{d1}}(f_1(x_v, x_3) - C_{ic}(x_3 - x_4) - A_1 x_2),$$

$$\dot{x}_4 = \frac{1}{A_2(L - y_0 - x_1) + V_{d2}}(-f_2(x_v, x_4) + C_{ic}(x_3 - x_4) - C_{ec}x_4 + A_2 x_2). \tag{6}$$

### 3.2. Stress Model of Drill Pipe Thread.

The stress analysis of drill pipe thread is shown in Figure 3, and the helix angle of drill pipe thread is shown in the following equation:

$$\alpha = \arctan\left(\frac{p}{\pi \cdot D}\right), \tag{7}$$

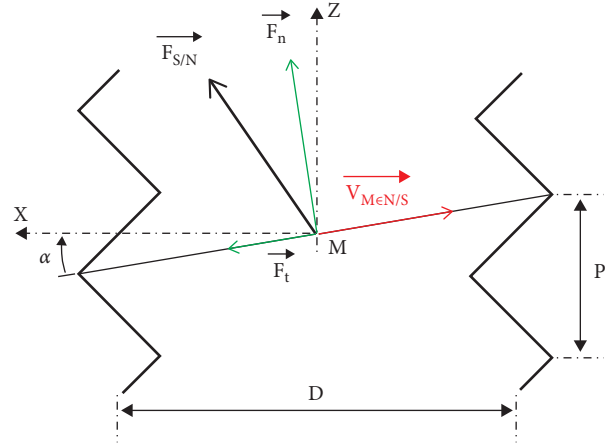where $p$ is the pitch and $D$ is the major diameter of the thread.

Equation (8) is the force perpendicular to the thread $F_n$, which depends on the relative displacement and speed between the nut and the screw:

$$F_n = d.v_{rel} + k \int v_{rel} dt, \tag{8}$$

where $k$ is the contact stiffness, $d$ is contact damping, and $v_{rel}$ is the relative linear velocity along the $Z$-axis.

From equations (9) and (10), the force on nut $F_{\text{nut}}$ and the torque on screw $T_{\text{screw}}$:

$$F_{\text{nut}} = F_n \cos \alpha - F_t \sin \alpha, \tag{9}$$

$$T_{\text{screw}} = \frac{D}{2} \left( F_n \sin \alpha + F_t \cos \alpha \right). \tag{10}$$

### 3.3. Elastic Model of Steel Wire Rope.

If the loading force is transmitted by steel wire rope, the steel wire rope has elastic deformation [12]. As shown in Figure 4, (11) is the kinematic equation [13]:

$$\left\{ m_2 \ddot{x}_2 - k(x_1 - x_2) = m_2 g, \, J_1 \ddot{\theta} + k(x_1 - x_2)r = F_q r, \right. \tag{11}$$

where $m_2$ is the load mass, $x_2$ is the load displacement, $x_1$ is the displacement of steel wire rope, $k$ is the elastic coefficient of steel wire rope, $J_1$ is the moment of inertia of the pulley, $R$ is the rotation radius of the pulley, $F_q$ is the starting force acting on the pulley, and $M_1 = F_q r$, $M_1$ is the pulley driving torque.

Equation (12) is the acceleration of steel wire rope:

$$\ddot{x}_1 = \ddot{\theta}r. \tag{12}$$

Combine equations (11) and (12) so that the elastic deformation of steel wire rope, $S = x_1 - x_2$, exports

$$\left\{ m_2 \ddot{x}_2 - kS = m_2 g, \, \frac{J_1}{r^2} \left( \ddot{S} + \ddot{x}_2 \right) + kS = F_q. \right. \tag{13}$$

Equation (14) is derived by operation transformation:

$$\ddot{S} + \frac{k\left(J_1/r^2 + m_2\right)}{m_2 J_1/r^2} S = \frac{\left(J_1/r^2 + m_2\right)}{J_1/r^2} m_2 g + F_s \frac{1}{J_1/r^2}, \tag{14}$$

where $F_s$ is the residual force, $Fs = Fq - m2g$:

$$\omega_n^2 = \frac{k\left(J_1/r^2 + m_2\right)}{m_2 J_1/r^2},$$

$$A = \frac{\left(J_1/r^2 + m_2\right)}{J_1/r^2}, \tag{15}$$

$$B = \frac{1}{J_1/r^2},$$

where $\omega_n$ is the natural frequency of the system. Then, equation (15) is obtained from equation (14):

$$\ddot{S} + \omega_n^2 S = A m_2 g + B F_s. \tag{16}$$

The kinematics equation of the system is obtained by solving equation (15), including displacement equation (16), velocity equation (17), and acceleration equation (18):

$$S = A \sin \omega_n t + B \cos \omega_n t + \frac{m_2 F_s}{k\left(m_2 + J_1/r^2\right)} + \frac{m_2 g}{k}, \tag{17}$$

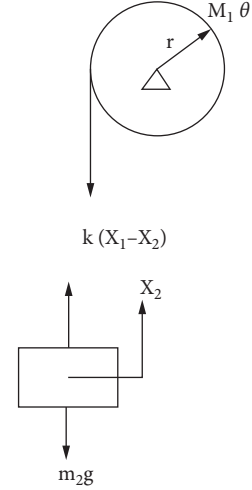$$\ddot{S} = A \omega_n \cos \omega_n t - B \omega_n \sin \omega_n t, \tag{18}$$



FIGURE 4: Suspension model of elastic steel wire rope.

$$\ddot{S} = -A \omega_n^2 \sin \omega_n t - B \omega_n^2 \cos \omega_n t. \tag{19}$$

When $t = 0$, it is the initial start; equations (19) and (20) are obtained:

$$S = \frac{m_2 g}{k},$$
$$\ddot{S} = 0, \tag{20}$$

$$A = 0,$$
$$B = -\frac{m_2 F_s}{k\left(m_2 + J_1/r^2\right)}. \tag{21}$$

Therefore, equations (16), (17), and (18) become equations (21), (22), and (23):

$$S = \frac{m_2 F_s}{k\left(m_2 + J_1/r^2\right)} \left(1 - \cos \omega_n t\right) + \frac{m_2 g}{k}, \tag{22}$$

$$\ddot{S} = \frac{m_2 F_s}{k\left(m_2 + J_1/r^2\right)} \omega_n \sin \omega_n t, \tag{23}$$

$$\ddot{S} = \frac{m_2 F_s}{k\left(m_2 + J_1/r^2\right)} \omega_n^2 \cos \omega_n t. \tag{24}$$

The kinematic equations of displacement, velocity, and acceleration of load obtained from equation (13) are equations (24), (25), and (26):

$$x_2 = \frac{F_s}{\left(m_2 + J_1/r^2\right)} \frac{t^2}{2} - \frac{F_s}{\left(m_2 + J_1/r^2\right)} \frac{1}{\omega_n} \left(1 - \cos \omega_n t\right), \tag{25}$$

$$\ddot{x}_2 = \frac{F_s}{\left(m_2 + J_1/r^2\right)} \left(t - \frac{1}{\omega_n} \sin \omega_n t\right), \tag{26}$$

$$\ddot{x}_2 = \frac{F_s}{\left(m_2 + J_1/r^2\right)} \left(1 - \cos \omega_n t\right). \tag{27}$$
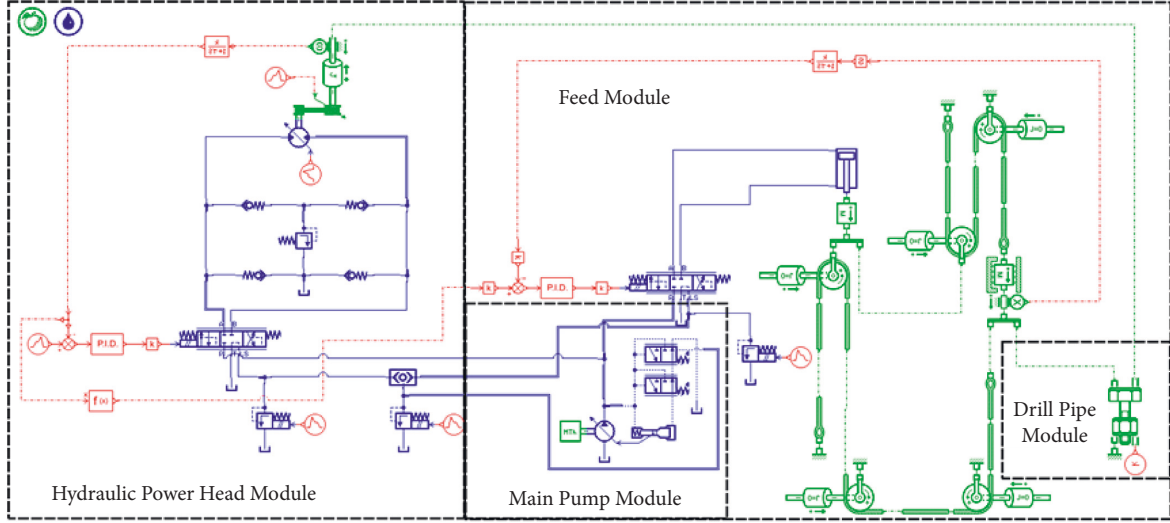
FIGURE 5: Simulation model of loading and unloading drill pipe.

TABLE 1: Simulation boundary parameters of the hydraulic system of the geological drilling rig.

| NO. | Parameter name (unit) | The set value |
|---|---|---|
| 1 | Maximum pressure of main pump (MPa) | 35 |
| 2 | Engine speed (r/min) | 2400 |
| 3 | Auxiliary pump displacement (mL/r) | 32 |
| 4 | Main pump displacement (mL/r) [15] | 74 |
| 5 | Volumetric efficiency of main pump [15] | 0.92 |
| 6 | Main pump mechanical efficiency [15] | 0.95 |
| 7 | Volumetric efficiency of auxiliary pump | 0.8 |
| 8 | Auxiliary pump mechanical efficiency | 0.95 |
| 9 | Feed cylinder diameter (mm) | 90 |
| 10 | Feed cylinder rod diameter (mm) | 70 |
| 11 | Feed cylinder stroke (mm) | 1125 |
| 12 | Maximum displacement of power head motor (mL/r) [14] | 80.4 |
| 13 | Minimum displacement of power head motor (mL/r) | 40 |
| 14 | Pressure difference between inlet and outlet of power head motor (MPa) | 24 |
| 15 | Power head motor 1 stage reduction ratio $I_0$ | 2.5 |
| 16 | Power head 1 gear reduction ratio $i_1$ | 15.625 |
| 17 | Power head 2 gear reduction ratio $i_2$ | 7.8125 |
| 18 | Power first 3 gear reduction ratio $i_3$ | 4.3925 |
| 19 | Power first 4 gear reduction ratio $i_4$ | 2.5 |
| 20 | Power head motor volume efficiency [14] | 0.95 |
| 21 | Power head motor mechanical efficiency [14] | 0.98 |
| 22 | Mechanical efficiency of power head reducer [14] | 0.98 |

Equation (27) is the transient force $F_2$ of steel wire rope:

$$F_2 = kS$$

$$= \frac{m_2 F_s}{\left(m_2 + J_1/r^2\right)} \left(1 - \cos \omega_n t\right) + m_2 g. \tag{28}$$

When, $\cos \omega_n t = -1$, $F_2 = F_{2\max}$, and

$$F_{2\max} = 2 \frac{m_2 F_s}{\left(m_2 + J_1/r^2\right)} + m_2 g. \tag{29}$$

TABLE 2: PID parameters in the simulation model.

| Module | P | I | D |
|---|---|---|---|
| Hydraulic power head module PID | 100 | 0 | 2 |
| Feed module PID | 100 | 0 | 1 |

According to (28), the maximum transient force $F_{2\max}$ of the steel wire rope is caused by the elastic coefficient $k$ of the steel wire rope, but the magnitude is independent of $k$. The transient force $F_2$ is a periodic motion force.
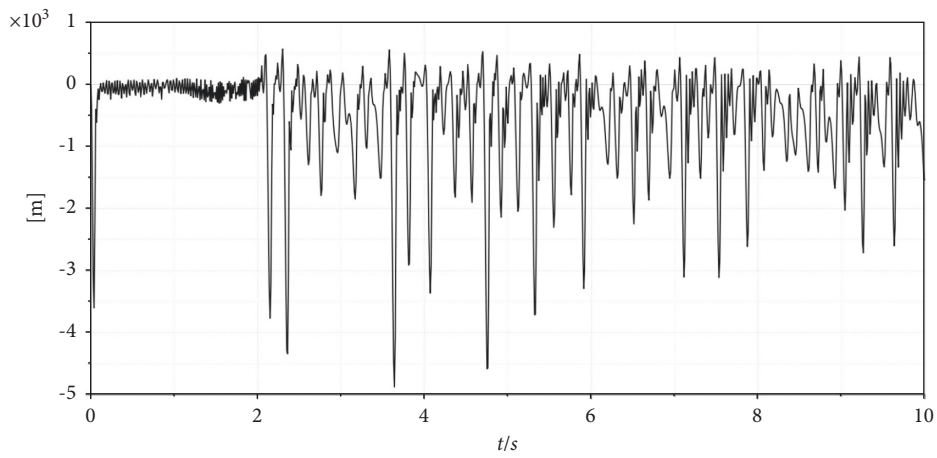
The displacement, velocity, and acceleration of load are periodic functions related to time.
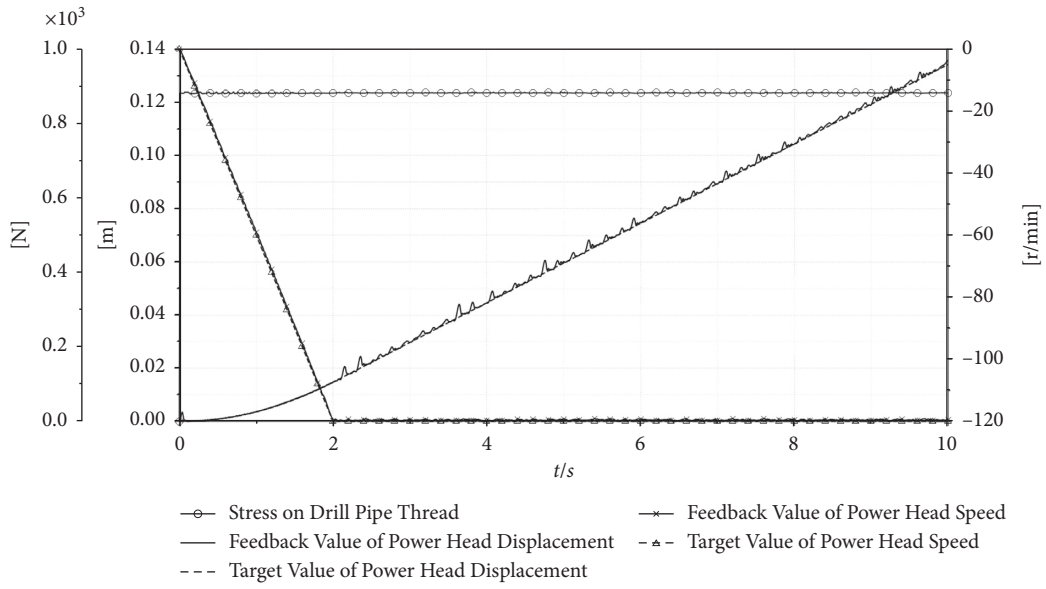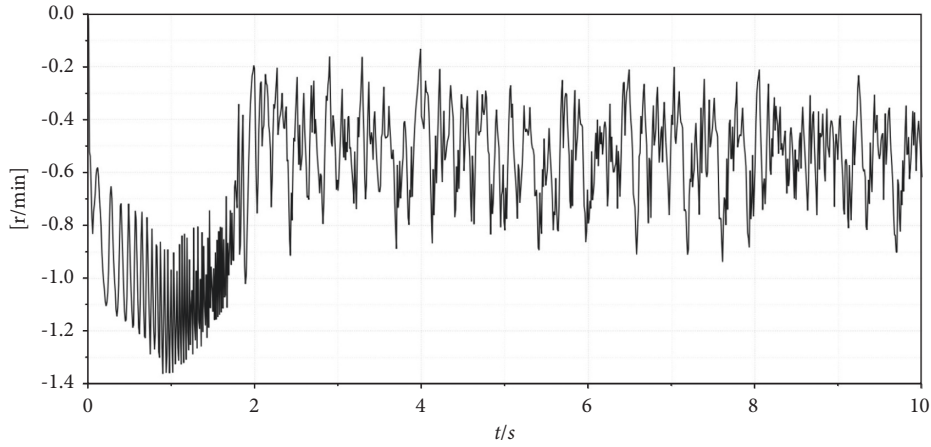
Figure 6: Simulation curve of loading and unloading drill pipe. (a) Simulation curve of loading and unloading drill pipe. (b) Error curve of powerhead speed. (c) Error curve of dynamic head displacement.
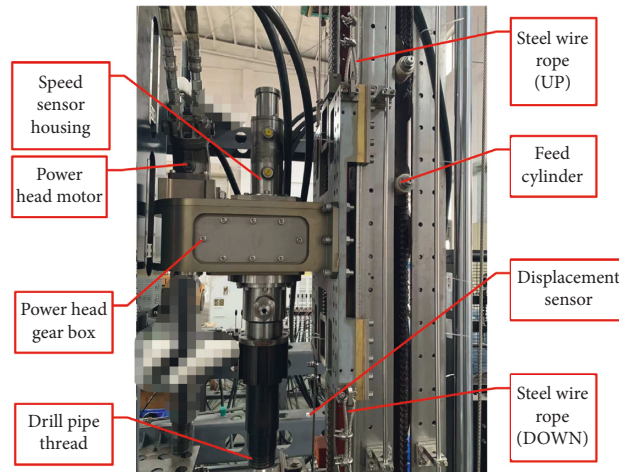
FIGURE 7: Application in subsea drilling rig.

TABLE 3: List of sensor parameters.

| Sensor name | Measurement parameters | Signal output type | Sensor accuracy | Sensor shape |
|---|---|---|---|---|
| Incremental encoder | Rotate speed | Pulse frequency | 360ppr |  |
| Displacement sensor | Displacement | 4–20 mA | 0.05% range |  |

## 4. Research on Modeling and Simulation

Using the established mathematical model, the AMESim model shown in Figure 5 is established according to the principle of Figure 1, and the simulation parameters are set according to the boundary of Table 1.

The loading and unloading drill pipe is simulated by AMSIM software. The power head speed control is the main control, and the feed cylinder control is the follow-up control. A PID controller [16, 17] is adopted for the speed and displacement of power head. The speed feedback value is converted into the displacement variable value of the power head by the controller and input into the PID controller of the feed cylinder. The displacement of the feed cylinder is controlled by the auxiliary valve. The PID parameters in Figure 5 are shown in Table 2.

It can be seen from Figure 6 that the power head drives the drill pipe from static to rotating speed of 120r/min, and the rotating speed is stable, as shown in Figure 6(a). The

speed control error is small, as shown in Figure 6(b). Affected by the elasticity of the steel wire rope, the displacement of the power head fluctuates periodically, as shown in Figure 6(c), and the displacement error curve of the power head, which is consistent with the kinematic equation of the steel wire rope elastic model, but has little effect on the force on the drill pipe thread, and the drill pipe thread is only affected by the gravity of the drill pipe. The simulation shows that the small flow valve core of the auxiliary valve can realize the closed-loop control of the screw thread loading and unloading drill pipe and avoid the screw thread damage caused by the control error through the connection of the steel wire rope, and the steel wire rope plays an elastic buffer role.

## 5. Practical Application

Applying the theory and scheme of this study on a 20m subsea drilling rig and using the compound action of power
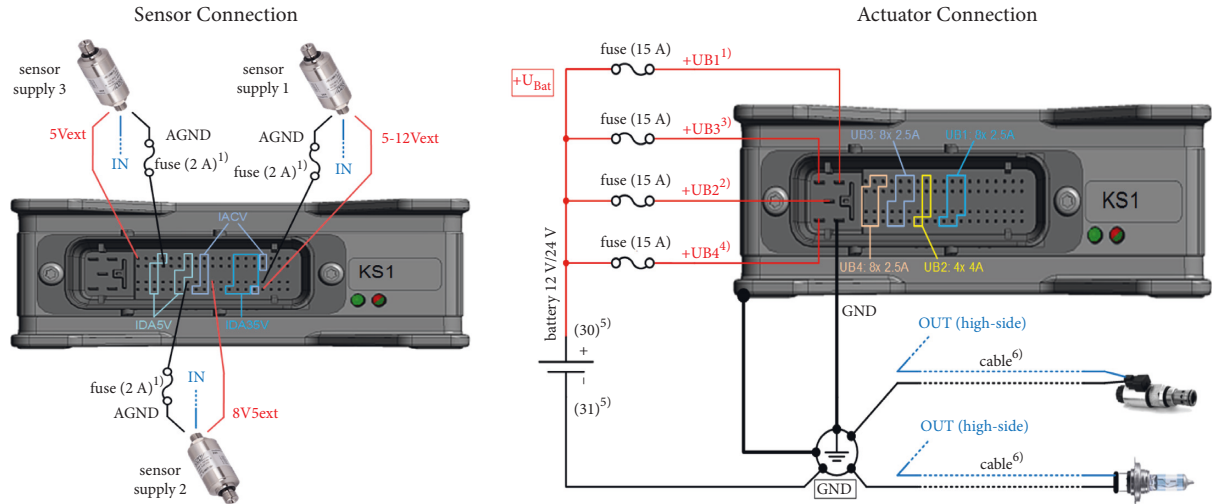
FIGURE 8: Wiring diagram of sensor and electric proportional valve [18].

head output drill pipe speed and power head displacement, through the drill pipe speed sensor and power head displacement sensor installed on the output side of the power head, as shown in Figure 7, the following control of power head displacement during drill pipe up and down is realized to effectively reduce the damage of drill pipe thread buckle.

The incremental encoder is selected to measure the drill pipe speed on the output side of the power head and installed in the speed sensor housing to prevent damage by seawater pressure. High precision pull wire displacement sensor is selected to measure the up and down displacement of the power head, and the encoder is encapsulated. The sensor parameters are shown in Table 3.

ESX-3CM special controller for construction machinery is selected for sensor signal acquisition and electric proportional valve control to build a closed-loop control. The sensor and electric proportional valve can be directly connected with the ESX-3CM controller, and the wiring mode is shown in Figure 8.

The ESX-3CM is a control and measurement unit. It is a control unit for managing sensors and actors within your system. The ESX-3CM is a control unit that consists of a modern and capable 32-bit architecture based on the Tri-Core TC1798 processor. The configured hardware is optimized for applications within mobile machines. Up to a total of 56 analog/digital input and outputs for measure and control is available for challenging tasks. [18].

## 6. Conclusion

In this study, the dynamics of drill pipe up and down shackle of the automatic geological drilling rig is studied. Starting from the hydraulic control system, the problem of thread buckle damage caused by excessive power head weight of geological drill pipe up and down shackle can be solved. The following conclusions can be drawn:

(1) The maximum transient force $F_{2\max}$ of the steel wire rope is caused by the elastic coefficient $k$ of the steel wire rope, but the magnitude is independent of $k$. The transient force $F_2$ is a periodic motion force. The displacement, velocity, and acceleration of load are periodic functions related to time.

(2) The installation of a small flow load-sensitive valve can accurately control the displacement of asymmetric hydraulic cylinder and then control the displacement of the power head. It has been well applied and verified in the subsea drilling rig project.

(3) The combined action of drill pipe speed and power head displacement is adopted, and the power head displacement is followed and controlled through drill pipe speed feedback. Combined with the feeding and loading of the drill rig power head, the steel wire rope is used to transfer the loading force, which can realize the automatic loading and unloading of drill pipe and effectively reduce the damage of drill pipe thread buckle.

## Data Availability

The data in the tables used to support the findings of this study are included within the article. The data in the figures used to support the findings of this study are available from the author (lzjcumtb@126.com) upon request.

## Conflicts of Interest

The authors declare that they have no conflicts of interest.

## References

[1] H. X. Shi, *Research on Thread Structure of Drill Pipe Connection*, China University of Geosciences, Beijing, China, 2017.

[2] C. Cai, *Stress Simulation Analysis and Gas-Sealing Capacity Researching of Casing Threaded Connection*, China University of Geosciences, Beijing, China, 2016.

 [3] W. Y. Wang, Y. X. Tang, and M. F. Zhu, *Drill Collar Thread Failure Analysis and Settle Measures*, Oil Field Equipment, Beijing, China, 2007.

 [4] A. R. Shahani and S. M. H. Sharifi, "Contact stress analysis and calculation of stress concentration factors at the tool joint of a drill pipe," *Materials & Design*, vol. 30, no. 9, pp. 3615–3621, 2009.

 [5] C. Santus, L. Bertini, M. Beghini, A. Merlo, and A. Baryshnikov, "Torsional strength comparison between two assembling techniques for aluminium drill pipe to steel tool joint connection," *International Journal of Pressure Vessels and Piping*, vol. 86, no. 2-3, pp. 177–186, 2009.

 [6] J. Van Wittenbergahe, P. De Baets, W. De Waele, and S. Van Autreve, "Numerical and experimental study of the fatigue of threaded pipe couplings," in *Proceedings of the 9th International Conference on Surface Effects and Contact Mechanics: Computational Methods and Experiments*, pp. 163–174, WIT Press, Southampton, UK, June 2009.

 [7] D. Croccolo, M. De Agostinis, and N. Vincenzi, "Failure analysis of bolted joints: effect of friction coefficients in torque-preloading relationship," *Engineering Failure Analysis*, vol. 18, no. 1, pp. 364–373, 2011.

 [8] T. T. Bui, G. De Roeck, J. Van Wittenberghe, E. Reynders, P. De Baets, and W. De Wim, "A modal approach to identify fatigue damage in threaded connections of large scale tubular strucures," in *Proceedings of the Internaional Conference on Noise and Vibration Engineering*, ISMA, Leuven, Belgium, July 2011.

 [9] S. X. Bai, ZH. J. Liu, and J. Wang, "Research on the dynamics of geological drilling rig against drill pipe impact," *Hindawi.Shock and Vibration*.vol. 2021, Article ID 6679169, 19 pages, 2021.

[10] ZH. J. Liu, *Research on Dynamic Characteristics of Working Device ofAutomatic Geological Drillig Rig Pipe Handling Systems*, China University of Geosciences, Beijing, China, 2019.

[11] H. E. Merritt, *Hydraulic Control System*, John Wiley & Sons, Hoboken, NJ, USA, 1967.

[12] M. J. Zhang and Q. Cao, *Dynamics of Construction Machinery*, National Defense Industry Press, Beijing, China, 2012.

[13] Q. Y. Liu, Q. H. Meng, and D. X. Pang, *Research and Application of Drilling System Dynamics Simulation*, Science Press, Beijing, China, 2009.

[14] Bosch Rexroth Company, *Mobile Machinery Hydraulic-Product Catalog-Part II-Hydraulic Motor-Reducer*, BoschRexroth Company, Lohra Main, Germany, 2014.

[15] Bosch Rexroth Company, *Mobile Machinery Hydraulic-Product Catalog-Part I-Hydraulic Pump*, Bosch Rexroth Company, Lohra Main, Germany, 2014.

[16] Bosch Rexroth Company, *Mobile Machinery Hydraulic-Product Catalog-Part III-Mobile Machinery Control Device*, Bosch Rexroth Company, Lohra Main, Germany, 2014.

[17] Z. J. Liu, B. L. Liu, and Y. B. Hu, *Fault Simulation of Hydraulic Winch System Stall. Hydraulic and Pneumatic*, Beijing, China, 2016.

[18] Sensor-Technik Wiedemann GmbH, *ESX-3CM CODESYS V3 User Manual*, Sensor-Technik Wiedemann, Kaufbeuren, Germany, 2017.